MODULI SPACES OF EMBEDDED CONSTANT MEAN CURVATURE SURFACES WITH FEW ENDS AND SPECIAL SYMMETRY

KARSTEN GROSSE-BRAUCKMANN AND ROBERT B. KUSNER

Abstract. We give sharp, necessary conditions on complete embedded CMC surfaces with three or four ends subject to reflection symmetries. The respective submoduli spaces are two-dimensional varieties in the moduli spaces of general CMC surfaces. Fundamental domains of our CMC surfaces are characterized by associated great circle polygons in the three-sphere.

We are interested in parametrizing the moduli space $\mathcal{M}_{g,k}$ of complete, connected, properly embedded surfaces in $\mathbb{R}^3$ with finite genus g and a finite number k of labeled ends having nonzero constant mean curvature. By rescaling we may assume this constant is 1, the mean curvature of the unit sphere. Two surfaces in $\mathbb{R}^3$ are identified as points in $\mathcal{M}_{g,k}$ if there is a rigid motion of $\mathbb{R}^3$ carrying one surface to the other. Moreover, we shall include in $\mathcal{M}_{g,k}$ a somewhat larger class of constant mean curvature (CMC) surfaces, the *almost* (or *Alexandrov*) *embedded* surfaces, which are immersed surfaces bounding immersions of handlebodies into $\mathbb{R}^3$. The space $\mathcal{M}_{g,k}$ is a finite dimensional real analytic variety, and in a neighborhood of a surface with no L^2-Jacobi fields it is a $(3k-6)$-dimensional manifold [KMP] for each $k \geq 3$.

A few of the CMC moduli spaces $\mathcal{M}_{g,k}$ are known explicitly: the only embedded compact CMC surface is a round sphere [A], so $\mathcal{M}_{g,0}$ is either a point ($g = 0$) or empty ($g > 0$); $\mathcal{M}_{g,1}$ is empty, since there are no one-ended examples [M]; two-ended examples are necessarily the Delaunay *unduloids* [KKS], which are simply-periodic surfaces of revolution whose minimal radius or *neckradius* $\rho \in (0, \frac{1}{2}]$ parametrizes $\mathcal{M}_{0,2}$, while $\mathcal{M}_{g,2}$ is empty for $g > 0$. The Kapouleas construction [Kp] shows that $\mathcal{M}_{g,k}$ is not empty for every $k \geq 3$ and every g. Furthermore, an embedded end of a CMC surface is asymptotically a Delaunay unduloid [KKS], and this defines in particular the neckradii and axes of the ends, which are related via a balancing formula. The Kapouleas examples all have very small neckradii, and it is an interesting problem to determine whether there are any constraints on which neckradii can be realized.

We call a CMC surface in $\mathcal{M}_{g,k}$ a *k-unduloid of genus g*, or simply *k-unduloid* if its genus is 0. The *triunduloids* of genus g comprising $\mathcal{M}_{g,3}$ are special in that *a priori* each has a plane of reflection symmetry [KKS], which we will think of as a *horizontal* plane. In the present paper we focus on CMC surfaces with such a horizontal reflection plane, along with $k-2$ extra *vertical* reflection planes: these yield two-dimensional submoduli spaces of $\mathcal{M}_{g,k}$. In particular, we study the Y-shaped *isosceles* triunduloids in $\mathcal{M}_{0,3}$, and the *rectangular* 4-unduloids in $\mathcal{M}_{0,4}$, having the extra vertical symmetry planes depicted in Figures 1(b) and 1(a), respectively.

Our main results here are sharp *a priori* bounds on the neckradii for these two symmetry types (Theorems 14 and 20). These bounds follow from an analysis of the noncompact CMC fundamental

1991 *Mathematics Subject Classification.* 53A10.

Supported by SFB 256 at Uni-Bonn, and NSF grant DMS 94-04278 at UMassAmherst and the IAS.

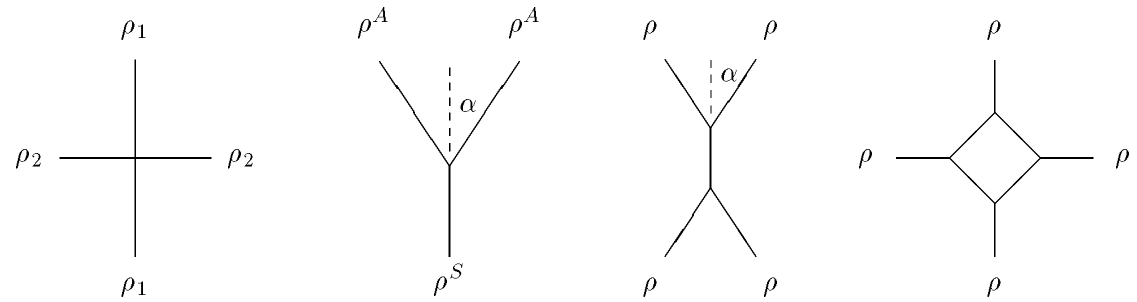

FIGURE 1. Axes and neckradii of rectangular, isosceles, and rhombic surfaces, as well as for a dihedrally symmetric 4-unduloid of genus 1.

domains and their associated boundary contours, using Lawson's theorem [L] [Ka]: a simply-connected fundamental domain of a CMC surface with the assumed reflection symmetries has an associated minimal surface in the three-sphere $\mathbb{S}^3$ whose boundary consists of great circle arcs and rays. This boundary contour in $\mathbb{S}^3$ can exist with only certain (asymptotic) edgelengths, and this limits the range of neckradii the asymptotically Delaunay ends can have. We also prove that, for given asymptotic axes of either symmetry type, there are exactly two associated spherical boundary contours for each neckradius below the maximal value, and exactly one at the maximum. We believe that each contour bounds a unique minimal surface in $\mathbb{S}^3$, so that our characterization of the family of spherical polygons should in fact be a characterization of the family of CMC surfaces for the given symmetry type.

One motivation for the present work is the behavior of a one-parameter family of dihedrally symmetric k-unduloids that was constructed in [G]; these surfaces have k asymptotic axes arranged in a plane with equal angles $2\pi/k$. Two dihedrally symmetric k-unduloids were shown to exist for neckradii in the interval $(0, \frac{1}{k})$ and one surface at the right endpoint. In fact, a completely different approach [KKn] showed that any k-unduloid with this symmetry had an upper bound on the neckradii which approached this $\frac{1}{k}$-bound for large k. These results suggested there might be some general constraints limiting the allowed neckradii of the ends, and restricting the number of CMC surfaces within these limits.

Although we do not prove the existence of complete CMC surfaces (with symmetries) in this paper, we do develop some tools which should aid in their construction, and a few comments about this are in order. First note that to construct a complete surface from a fundamental domain involves a period problem. For isosceles triunduloids it is remarkable that the known asymptotics of each end, together with the balancing formula, suffice to solve the period problem; for rectangular 4-unduloids, the period problem is solved by symmetry alone. This is no longer true for some closely related symmetry types of surfaces, like the *rhombic* 4-unduloids (see Figure 1(c)) and dihedrally symmetric k-unduloids of genus 1 (Figure 1(d)); their period problems can still be solved experimentally [GP]. The existence and uniqueness questions for these symmetry types, along with the problem of the general triunduloid, will be addressed elsewhere [GKS].

Finally, we point out a particularly interesting feature of the isosceles family (Subsection 5.5.4): as one follows a loop of isosceles triunduloids winding around the point of isosceles moduli space corresponding to a surface with a cylindrical "stem" end, bubbles are generated or deleted on the stem. Similarly, in the rhombic case there is a finite middle segment which can have cylindrical neckradius: looping around on nearby surfaces in $\mathcal{M}_{0,4}$ adds or deletes bubbles on this segment. Since it was expected that components of the moduli space $\mathcal{M}_{0,k}$ would be indexed by the number of bubbles along such finite segments, these observations lead us to conjecture that $\mathcal{M}_{0,k}$ is always connected.

1. Preliminaries

1.1. **Lawson's theorem.** Our main tool is this consequence of Bonnet's fundamental theorem, as formulated by Lawson [L, p.364]:

Theorem 1. *Let $\tilde{M}$ be a simply connected immersed minimal surface in $\mathbb{S}^3$. Then there exists an isometric immersed* CMC *surface $M \subset \mathbb{R}^3$, and vice versa. Furthermore, a planar arc of (Schwarz) reflection in M corresponds to a great circle arc in $\tilde{M}$.*

We call $\tilde{M}$ and M *conjugate cousin surfaces* or simply *associated surfaces*.

We will consider fundamental domains of CMC surfaces with respect to a group of reflections, whose entire boundary consists in planar arcs of reflection symmetry (geodesic curvature arcs).

Corollary 2. *A simply connected* CMC *surface M bounded by geodesic curvature arcs is associated to a spherical minimal surface $\tilde{M}$ bounded by great circle arcs.*

The fundamental domains of the finite topology CMC surfaces we study are not compact, and some bounding geodesic curvature arcs are infinitely long. We call such an arc a *ray* or a *line* if it extends in one or both directions to infinity, respectively. We use the same terminology for the boundary of the associated minimal domains in $\mathbb{S}^3$: each arc of the boundary is a parameterized great circle arc, which in the case of rays and lines covers the great circle infinitely many times.

1.2. **Karcher's Hopf fields.** A *Hopf field* is defined by the oriented unit tangent vectors to the great circle fibres of a fixed, oriented Hopf fibration of $\mathbb{S}^3$. Each oriented great circle is tangent to a unique Hopf field. Since there is an $\mathbb{S}^2$ worth of fibres in a Hopf fibration, and since the space of oriented great circles in $\mathbb{S}^3$ is $\mathbb{S}^2 \times \mathbb{S}^2$, there is an $\mathbb{S}^2$ worth of such fibrations. Each fibration can be identified with a tangent direction at some point p in $\mathbb{S}^3$. In the following A, B, C will always denote a fixed positively oriented orthonormal basis of the tangent space $T_p\mathbb{S}^3 = \mathbb{R}^3$. With these choices, a Hopf field is determined by a linear combination $aA + bB + cC$ with $a^2 + b^2 + c^2 = 1$.

The spherical boundary contours associated to a CMC fundamental domain bounded by geodesic curvature arcs have a property independent of the length of the arcs: each arc of the contour determines a Hopf field. More precisely the Hopf fields are unique with the following properties: (i) fields determined by consecutive great circle arcs make an angle equal to the angle enclosed by the geodesic curvature arcs at a vertex (this is the dihedral angle of the two symmetry planes containing the arcs); (ii) when measured in terms of Hopf fields, the tangent plane along the boundary of the spherical minimal surface rotates from one vertex to the next as much as the tangent plane rotates between two vertices on the CMC domain.

Hopf fields were added to Lawson's conjugate surface construction by Karcher. See [Ka] or [G] for proofs and details.

1.3. **Ends.** Suppose we divide a CMC surface by its reflection symmetry group. If a symmetry plane contains the axis of an end, we call the portion to one side of this plane a *half end.* If another symmetry plane contains the axis and is orthogonal to the first plane, then the portion contained in the wedge between these planes is a *quarter end.*

We want to characterize the pair of rays on the boundary of quarter or half ends. To do this we look at the case of a quarter or half Delaunay surface first. A quarter end of a Delaunay unduloid with neckradius ρ has an associated boundary polygon with two great circle rays; the associated spherical minimal surface domain, which is part of a *spherical helicoid*, contains perpendicular great circle arcs of length

$$\frac{\pi\rho}{2} \quad \text{and} \quad \frac{\pi(1-\rho)}{2}. \tag{1}$$

Similarly a half end has perpendiculars of length

$$\pi\rho \quad \text{and} \quad \pi(1-\rho). \tag{2}$$

Since associated surfaces are isometric, this follows from the fact that there are symmetry circles of radius ρ and $1-\rho$ running around a neck or bulge of the unduloid, respectively. These circles alternate at distance $\pi/2$ for $\rho \neq 1/2$; in case $\rho = 1/2$ the surface associated to the cylinder is foliated by these perpendiculars (it is contained in a Clifford torus).

An end of an almost embedded CMC surface with finite topology is asymptotically a Delaunay unduloid [KKS], so its neckradius and axis are defined. It turns out that the great circle rays bounding quarter and half ends coincide with the rays on the boundary associated to the limiting quarter and half Delaunay ends.

Lemma 3. *Let M be a CMC fundamental domain which contains a quarter end of neckradius ρ. The associated minimal domain $\tilde{M}$ in $\mathbb{S}^3$ is then bounded by two great circle rays. The asymptotic limit of the surface contains perpendicular great circle arcs of lengths given as in* (1)*. Similarly, a half end of neckradius ρ is bounded by two great circle rays, and its asymptotic limit contains perpendiculars of lengths given as in* (2)*.*

Proof. By Lawson's theorem $\tilde{M}$ has great circle boundary rays. Each embedded end of M is exponentially asymptotic (in the C^∞-topology – see Subsection 1.4 below) to a Delaunay unduloid [KKS]. Thus $\tilde{M}$ is asymptotic to a spherical helicoid. A great circle ray asymptotic to a great circle must actually cover the great circle. Hence the boundary rays of $\tilde{M}$ are the great circle rays bounding the associated limiting spherical helicoid. □

1.4. **Continuity of families.** We define a topology on the set of great circle q-gons with fixed Hopf fields by taking the set of arclengths in $\mathbb{R}^q_+$ as continuous coordinates. We will also need a topology on families of polygonal contours containing a consecutive pair of rays. The pair will always have a shortest perpendicular tangent to a given Hopf direction. In this case we can truncate the rays at the endpoints of this perpendicular, and include their truncated lengths (modulo 2π), as well as the length of this perpendicular into the coordinates.

Given a CMC surface M we can write sufficiently C^0-close CMC surfaces as graphs over M and consider the C^1-norm of these graphs. By elliptic regularity, the resulting topology is equivalent to the C^∞-topology. This is the topology we would like to use, though for noncompact M there are some additional subtleties, since a surface we may wish to consider as "close" to M may not necessarily be C^0-close at the ends. Nevertheless, using the asymptotic behavior [KKS] it is possible to define a natural topology on families of noncompact CMC surfaces by declaring noncompact surfaces to be "close" if they also have closeby asymptotic axes and Delaunay neckradii – a detailed formulation is presented in Section 2 of [KMP]. Using this topology, and Lawson's theorem above, we obtain the following fact.

Lemma 4. *Consider a family of* CMC *surfaces invariant under a fixed group of reflections, such that their fundamental domains are simply connected and bounded by geodesic curvature arcs. The map, which assigns to these surfaces the great circle polygons bounding the associated minimal domains, is continuous.*

1.5. **Balancing and Kapouleas' existence result.** Let us associate a *force* vector

$$f := 2\pi\rho(1-\rho)a \in \mathbb{R}^3 \tag{3}$$

to a Delaunay unduloid with neckradius ρ, whose axis points in the direction of the unit vector a. Similarly, for each end of a surface in $\mathcal{M}_{g,k}$, the asymptotic Delaunay limit defines neckradii and axes, and hence forces $f_1, \dots, f_k$. The *balancing formula*

$$\sum_{i=1}^{k} f_i = 0, \tag{4}$$

is a necessary condition, which in fact holds in much greater generality [KKS].

It is a deep fact that balancing is also, in a certain sense, a sufficient condition for the existence of CMC surfaces: among Kapouleas' results [Kp] is that k-unduloids exist for a dense set of asymptotic axis directions whose force vectors $f_1, \dots, f_k$ are balanced and small. This smallness condition means that the neckradii are also small. Of course, here our aim is to study phenomena which occur for large neckradii.

2. Reflection symmetry

2.1. **Alexandrov reflection.** A. D. Alexandrov [A] invented a reflection method which was first applied to show that the round sphere is the only *compact* (almost) embedded CMC surface. This reflection principle was generalized [KKS] to noncompact CMC surfaces in $\mathbb{R}^3$, and can be stated in the following detailed form:

Theorem 5. *Let M be an almost embedded, complete* CMC *surface of finite topology. If M lies in a planar slab of finite thickness, then there is a plane P in this slab which is a symmetry plane for M. Furthermore, each symmetric open half M^+ and M^- of M is locally a graph lying to one side of P. More precisely, viewing M as the isometric immersion I of an abstract surface Σ, we can take $\Sigma = \bar{\Sigma}^+ \cup \bar{\Sigma}^-$ with $M^\pm = I(\Sigma^\pm)$. The restriction of I to $\Sigma^\pm$ can then be written in the form $I = (\iota, \pm u)$ where u is a positive function over some surface domain U, and ι is an isometric immersion of U into P. In case M is embedded, we may take $M = \Sigma$ and $U \subset P$, so that each half $M^\pm$ is globally a graph; in general, however, U need not be a planar domain.*

Let us prove that $M^\pm$ lies to one side of P; all other statements are proved in Remark 2.13 of [KKS]. The boundary $\partial M^\pm$ is contained in P, that is, $u = 0$ on ∂U. By the asymptotics u actually takes a minimum. Suppose that this minimum value is negative. Since M^+ is locally a graph its mean curvature vector points downward. Using a plane parallel to P as a comparison leads to a contradiction.

Since each end of an almost embedded CMC surface with finite topology is asymptotically Delaunay, the previous theorem applies even when only the configuration of the axes is known.

Corollary 6. (i) *If the axes of the ends of M are contained in a slab then M has a symmetry plane P parallel to the bounding planes of the slab.*
(ii) *If M has all its axes parallel, then M is a Delaunay unduloid.*

For part (ii), the above argument now shows that M must be cylindrically bounded, that is, within a bounded distance of a line. This means we can apply the reflection argument of the theorem in any direction about this line, and conclude that M is a surface of revolution about an axis parallel to this line.

2.2. **Schwarz reflection.** If we have a CMC surface M with reflectional symmetries then we can recover it by Schwarz reflection from a fundamental domain bounded by geodesic curvature arcs. In the situation of the above theorem, because $M^\pm$ is to one side of the horizontal symmetry plane P, the intersection $M \cap P$ consists of geodesic curvature arcs. We are interested in what happens when further symmetry planes are present. In particular we consider a *vertical* symmetry plane V, which is a plane orthogonal to the *horizontal* symmetry plane P.

The vertical reflection acts isometrically on the abstract surface Σ with a fixed point set F, and again $I(F) \subset V \cap M$ consists of geodesic curvature arcs. In the embedded case $I(F) = V \cap M$.

When M has genus 0 and k ends we can represent Σ^+ (or Σ^-, or even U) by a closed disk D with k points removed from ∂D corresponding to the ends of M. Furthermore, if we take a conformal representation, then an isometry of Σ^+ acts by a hyperbolic isometry of D. Thus the fixed point set $F^+ = F \cap \Sigma^+$ of a reflection is a hyperbolic geodesic. This geodesic joins either a pair of boundary punctures, or a boundary point and a puncture, or a pair of boundary points. The corresponding cases on M^+ are either a geodesic curvature line, or a ray, or an arc, respectively.

For genus 1 we can replace the disk representing M^+ with an annulus, whereas for genus $g > 1$ we must allow for h handles attached to the disk as well as c open disks removed from the interior of D, where $g = c + 2h$. Note that U is a planar domain if and only if $h = 0$.

We summarize our discussion above as follows.

Lemma 7. *For almost embedded k-unduloids M of genus* 0*, under the assumption of (horizontal) coplanar ends, the fixed point set F^+ under reflection in a vertical mirror plane V is connected and is either an arc in $M^+ \cap V$ from the horizontal plane P to itself, a ray from P to an end, or a line from one end to another.*

3. The trigonometry of Lawson quadrilaterals

3.1. **Existence.** Our analysis rests on spherical trigonometry, namely the trigonometry of the boundary polygons of the spherical minimal surfaces associated to the fundamental domains for

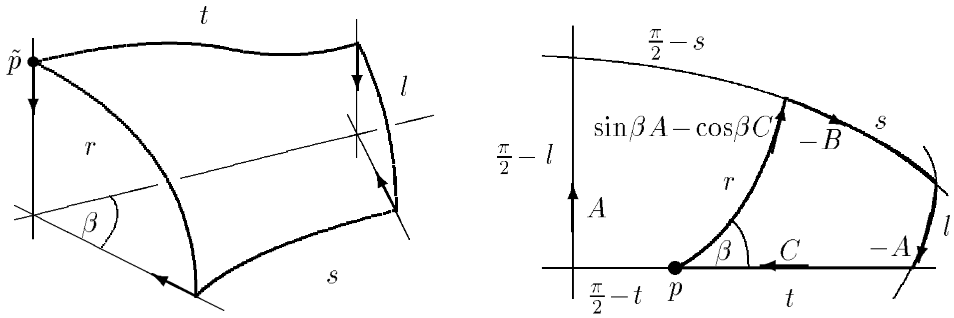

FIGURE 2. Quadrilateral bounding a Euclidean CMC fundamental domain and an isometric spherical minimal domain (righthand sketch is meant as a stereographic projection).

the CMC surfaces with few ends. The basic polygon for our analysis is a quadrilateral in $\mathbb{S}^3$ with Hopf fields $-A$, C, $\sin\beta\, A - \cos\beta\, C$, $-B$. Such a quadrilateral has three right angles, and one oriented angle $\beta \in [0, 2\pi)$ enclosed by the C- and $(\sin\beta\, A - \cos\beta\, C)$-arc at some point p.

We will use the letters l, t, r, s to denote the lengths of a quadrilateral as in Figure 2. We call quadrilaterals with the described Hopf fields, positive lengths, and $0 < l \leq \pi/4$ *Lawson quadrilaterals.* We denote them $\Gamma(l, t, r, s; \beta)$. They arise from the truncation of associated quarter ends with an asymptotic perpendicular of length l given by Lemma 3; if we choose the shorter perpendicular then indeed $0 < l \leq \pi/4$. The Lawson quadrilaterals are the associated boundaries of CMC fundamental domains coming from doubly periodic CMC surfaces provided $\beta = \pi/3$, $\pi/4$, or $\pi/6$ (see [L] or [G]).

In this section we classify all Lawson quadrilaterals. We first construct two basic families of quadrilaterals with edge lengths at most π and then extend them to obtain all quadrilaterals. The family (i) in the following lemma was already described in Lemma 3.1 of [G].

Lemma 8. *For each $\beta \in (0, \pi/2) \cup (\pi/2, \pi)$ there exists a continuous one-parameter family of Lawson quadrilaterals $\Gamma(l, t, r, s; \beta)$ as follows:*
(i) If $0 < \beta < \pi/2$ the lengths l, t, r, s range from $0, 0, 0, 0$ past $\beta/2, \pi/4, \pi/4, \beta/2$ to $0, \pi/2, \pi/2, \beta$. Here r, s, t are monotonic, whereas l monotonically increases on the first part of the family and monotonically decreases on the second half.
(ii) If $\pi/2 < \beta < \pi$ the lengths l, t, r, s range from $0, \pi, 0, \pi$ past $\beta/2, 3\pi/4, \pi/4, \pi - \beta/2$, to $0, \pi/2, \pi/2, \pi - \beta$. Again r, s, t are monotonic, whereas l monotonically increases on the first part of the family and monotonically decreases on the second half.

Proof. A Lawson quadrilateral with $0 < l, t, s < \pi/2$ and $0 < r, \beta < \pi$ is uniquely characterized by the four formulas

$$\cos s \cos r = \cos l \cos t, \tag{5}$$

$$\sin s \cos r = \sin l \sin t, \tag{6}$$

$$\cos s \cos l = \cos r \cos t + \cos\beta \sin r \sin t, \tag{7}$$

$$\sin s \sin l = \cos r \sin t - \cos\beta \sin r \cos t. \tag{8}$$

These four formulas can be obtained using the spherical cosine law, and each is implied by the remaining three, so that one parameter is free. Indeed for $0 < l, t, r, s, \beta < \pi/2$ it is shown in [G] that the three equations

$$\tan s = \tan l \tan t, \tag{9}$$

$$\tan 2t = \cos\beta \tan 2r, \tag{10}$$

$$\cos 2l = \sqrt{\cos^2\beta \sin^2 2r + \cos^2 2r}, \tag{11}$$

are equivalent to (5) – (8) except in case $r = \pi/4 \Leftrightarrow t = \pi/4 \Leftrightarrow l = \beta/2 \Leftrightarrow s = \beta/2$. For all other $0 < r < \pi/2$ we get a length $0 < l \le \beta/2$ by (11), $0 < t < \pi/2$ by (10) and $0 < s < \pi/2$ by (9). This gives a continuous family of quadrilaterals for which (5) – (8) hold, so that part (i) is proved.

To prove (ii) note that $0 < l, t, r, s, \beta < \pi/2$ solve (5) – (8) if and only if $\Gamma(l, \pi - t, r, \pi - s; \pi - \beta)$ is a Lawson quadrilateral. To see this we extend Figure 2(b) to the left up to the next perpendicular of length l. Then the extended part plus the portion to the left of the bold quadrilateral form together a large quadrilateral. Up to the motion $(A, B, C) \mapsto (A, -B, -C)$ this quadrilateral has exactly the Hopf fields of the bold quadrilateral, but $\pi/2 < \beta < \pi$. Thus it is a Lawson quadrilateral, and the claims for (ii) follow from (i). □

The case $\beta = \pi/2$ is somewhat different. The equations (5) – (8) can be checked directly to confirm the existence of the following Lawson quadrilaterals with lengths at most π.

Lemma 9. *There exist right-angled Lawson quadrilaterals* $\Gamma(l, t, r, s; \pi/2)$
(i) *with* $0 < l \le \pi/4$, $r = \pi/2 - l$, *and constant lengths* $s = t = \pi/2$,
(ii) *with* $0 < l = r \le \pi/4$, *and* $s = t = \pi$, *and*
(iii) *with* $l = r = \pi/4$, *and* $0 < s = t$.

These right-angled quadrilaterals bifurcate, for instance at $\Gamma(\pi/4, \pi/2, \pi/4, \pi/2; \pi/2)$, which is of type (i) and (ii). As Figure 2 indicates, the right-angled Lawson quadrilaterals are the associated boundaries of fundamental domains for the Delaunay unduloids. Therefore these bifurcations can be given the following geometrical interpretation. For the non-cylindrical unduloids the planar curvature circles are spaced with distance $\pi/2$ along the meridians. Small and large circles alternate, so that at distance $\pi/2$ there are two different circles (case (i) of the Lemma), and at distance π two equal ones (case (ii)). On the cylinder, there is a continuous family of planar symmetry circles having any distance $s = t > 0$ (case (iii)).

3.2. **Uniqueness.** We now want to characterize all Lawson quadrilaterals. In the general case $l, t, r, s \in \mathbb{R}_+$ the 'quadratic' equations (9) – (11) imply (5) – (8) only up to sign. Checking cases for the latter set of equations gives the uniqueness result:

Lemma 10. *All Lawson quadrilaterals with* $0 \le \beta < \pi$ *are generated from those listed in Lemma 8 and 9 by the following substitutions:*
(i) *adding* $2\pi n$ *for* $n \in \mathbb{N}$ *to* r, s, *or* t;
(ii) *replacing* (s, t) *by* $(s + \pi, t + \pi)$;
(iii) *replacing* (r, t) *by* $(r + \pi, t + \pi)$;
(iv) *replacing* (r, s) *by* $(r + \pi, s + \pi)$.

Whereas there are no Lawson quadrilaterals with $\beta = \pi$, the quadrilaterals with $\pi < \beta < 2\pi$ are obtained by another substitution from Lemma 10:

Lemma 11. *Lawson quadrilaterals with $\pi < \beta < 2\pi$ are obtained from Lemma 8 and 9 using the following substitutions:*
(i) replacing (r, β) by $(2\pi - r, \beta + \pi)$, or
(ii) replacing (r, s, β) by $(\pi - r, s + \pi, \beta + \pi)$.
All such quadrilaterals are obtained from these by the substitutions listed in Lemma 10.

4. Rectangular surfaces

Consider 4-unduloids of arbitrary genus with three orthogonal symmetry planes. For combinatorial reasons the axes of the ends must all be contained in one of the planes, which we call horizontal. On the other hand, by balancing and Corollary 6(ii) no two axes coincide, and there are only two ways for a 4-unduloid to have this symmetry:

- The axes form a right-angled cross, so that they are contained in the intersection of the horizontal with the vertical symmetry planes as in Figure 1(a). Opposite ends are congruent and thus there are only two neckradii ρ_1 and ρ_2. Since the axes are at right angles to each other we call such 4-unduloids *rectangular*.
- All ends are congruent and their axes form an angle α or $\pi/2 - \alpha$ with the intersection of the two vertical symmetry planes as in Figure 1(c). There can be a finite length segment in between the intersection of two pairs of the four axes. We call this case *rhombic*.

The two cases have the dihedrally symmetric 4-unduloids [G] in common.

We assume our surfaces have genus 0 for the remainder of this section. In our conformal model given in Subsection 2.2 we can represent each half of a four-ended surface by a closed disk with four boundary punctures. One vertical reflection can either (i) fix a pair of opposite punctures and interchange the other, or (ii) induce a transposition of two pairs of punctures. The fixed point set under the vertical reflection joins the fixed punctures in case (i), and by Lemma 7 there is a geodesic curvature line on each half of the CMC surface. In case (ii) the fixed point set is a geodesic curvature arc which under the horizontal reflection completes to a closed loop.

Any other vertical reflection must be of the same type, unless the surface is dihedrally symmetric. Thus case (i) corresponds to the rectangular surfaces, while (ii) is the rhombic case. In particular, a rectangular surface has a fundamental domain bounded by one line and two rays meeting in a right angle at a point $\tilde{p}$ as in Figure 3(a). On the other hand, a rhombic surface has fundamental domain bounded by two arcs and two rays, all meeting at right angles. The rectangular case, which we consider here, does not pose a period problem; the period problem posed by the rhombic surfaces can be dealt with numerically [GP].

The rectangular fundamental domain contains two quarter ends. To simplify we use asymptotic perpendiculars provided by Lemma 3 to truncate the spherical contour. We truncate at the necks, and by (1) the truncated arcs have lengths

$$0 < l_1, l_2 \leq \pi/4. \tag{12}$$

The resulting pentagon, with the truncated line of length s and two truncated rays of lengths t_1, t_2, is right-angled. We denote it by $\Gamma(t_1, l_1, s, l_2, t_2)$.

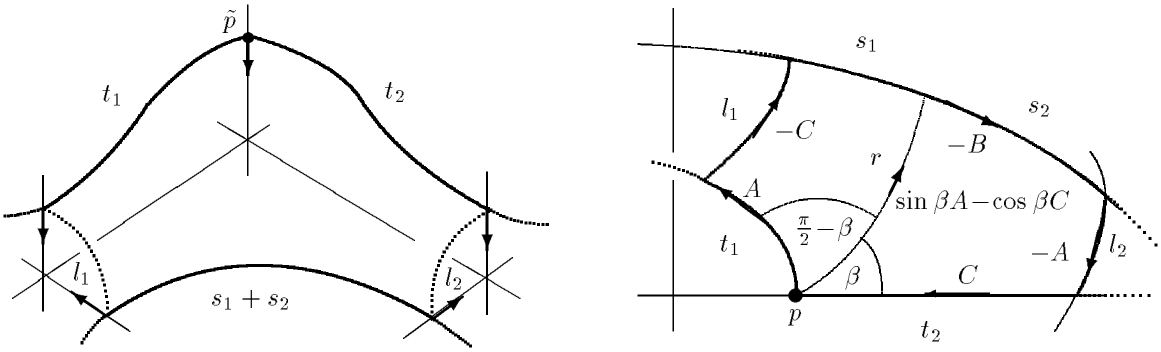

FIGURE 3. Generating CMC fundamental domain for a rectangular surface, and spherical boundary polygon of associated spherical minimal surface. The spherical contour is truncated by two asymptotic perpendiculars which are associated to the two dotted symmetry lines of length l_1, l_2 contained in the asymptotic CMC limit of the end.

To reduce the spherical trigonometry of these pentagons to the quadrilaterals of Section 3 we determine the Hopf fields of the pentagons (Figure 3). We start at the intersection point p of the geodesic rays. The Hopf fields are then A for one ray, $-C$ for its asymptotic perpendicular, $-B$ for the line, $-A$ for the other asymptotic perpendicular, and C for the returning ray. We refer to a right-angled pentagon with these Hopf fields and positive lengths satisfying (12) as a *truncated rectangular contour*. The main geometric observation is a decomposition of these pentagons into quadrilaterals as indicated in Figure 3(b):

Lemma 12. *The set of truncated rectangular contours* $\Gamma(t_1, l_1, s, l_2, t_2)$ *is in 1-1 correspondence to pairs of Lawson quadrilaterals* $\Gamma_1(l_1, t_1, r, s_1; \beta)$ *and* $\Gamma_2(l_2, t_2, r, s-s_1; \pi/2-\beta)$ *with* $0 < r, \beta < \pi/2$.

Proof. If the two quadrilaterals are glued along their arcs of length r in such a way that the two complementary angles face each other and are contained in the same tangent plane, a right-angled pentagon is formed. Moreover, this pentagon has the desired Hopf fields.

On the other hand, suppose the pentagon is given. We consider a great circle through p which meets the geodesic containing the opposite $-B$ arc orthogonally in a point q. Extending s and t_1, t_2 further if necessary, two quadrilaterals Γ_1 and Γ_2 result. By orthogonality, the Hopf field of the diagonal is of the form $\sin\beta\, A - \cos\beta\, C$ with $\beta \in (0, 2\pi)$. We claim that in fact $0 < \beta, r < \pi/2$.

We use the following fact, which is immediate from Lemmas 8, 10, and 11: a Lawson quadrilateral with $\beta \in (0, \pi)$ and $\beta \neq \pi/2$ has $0 < r \bmod \pi < \pi/2$, whereas a quadrilateral with $\beta \in (\pi, 2\pi)$ and $\beta \neq 3\pi/2$ has $\pi/2 < r \bmod \pi < \pi$.

Suppose that the quadrilateral Γ_2 has $\beta \in (\pi/2, \pi)$. This means that the quadrilateral Γ_1 has angle in $(3\pi/2, 2\pi)$. By the preceding fact there is no consistent choice of r and this case is impossible. The same argument applies to $\beta \in (3\pi/2, 2\pi)$. The case $\beta \in (\pi, 3\pi/2)$ leads to a consistent choice $r \in (\pi/2, \pi)$. However, in this case we can replace the diagonal by an arc in the opposite direction; the arc in the opposite direction has $\beta \in (0, \pi/2)$ and meets the antipodal point of the former endpoint at a length $\pi - r \in (0, \pi/2)$. Finally, since $l_1, l_2 > 0$ the angle β can not be an integer multiple of $\pi/2$, and hence the claim is proved.

As $\beta \in (0, \pi/2)$, the length of r can be taken to be in $(0, \pi/2)$ by Lemma 8(i) and Lemma 10. Furthermore, again by Lemma 10 we see that q is contained in the pentagon and the extension is not necessary. □

We now analyze the pentagons via the two quadrilaterals of the lemma. Note that the family of dihedrally symmetric 4-unduloids constructed in [G] satisfies $0 < \rho \leq 1/4$. These surfaces lead to symmetric pentagons $\Gamma(l, t, s, t, l)$ with $0 < l \leq \pi/8$; they decompose into two equal Lawson quadrilaterals $\Gamma(l, t, r, s/2; \pi/4)$ as given by Lemma 8(i). For the general case the two quadrilaterals are different but $l_1 + l_2 \leq \pi/4$ still holds.

Lemma 13. *There exists a continuous two-parameter family of truncated rectangular pentagon contours*

$$\mathcal{G}_{\text{trunc}} = \{\Gamma(t_1, l_1, s, l_2, t_2) \mid 0 < l_1, l_2 \text{ and } l_1 + l_2 \leq \pi/4,\ 0 < t_1, t_2, s < \pi/2\}.$$

For each pair $l_1, l_2 > 0$ with $l_1 + l_2 < \pi/4$ the family contains exactly two distinct contours, while for $l_1 + l_2 = \pi/4$ there is only one.

Proof. We determine a quadrilateral $\Gamma_1(l_1, t_1, r, s_1; \beta)$ with angle $0 < \beta < \pi/2$ and all edgelengths in $(0, \pi/2)$ as follows. We take $0 < l_1 < \pi/4$ and r with $l_1 < r < \pi/2 - l_1$ as parameters. Then (11) (with $l = l_1$) gives

$$\cos^2\beta = \frac{\cos^2 2l_1 - \cos^2 2r}{\sin^2 2r} \tag{13}$$

and we obtain a $\beta \geq 2l_1$. Since $l_1 < r$ the numerator of (13) is positive, and the fraction is at most 1, so that we can choose $\beta < \pi/2$. Then Lemma 8(i) gives existence of a family of quadrilaterals $\Gamma_1(l_1, t_1, r, s; \beta)$ with $0 < t_1 = t < \pi/2$ and $0 < s < \beta < \pi/2$ as in (10) and (9). These quadrilaterals depend continuously on the parameters r and l_1.

With r and β fixed, we now construct another quadrilateral $\Gamma_2(l_2, t_2, r, s - s_1; \pi/2 - \beta)$. According to (11) and Lemma 8(i) there is such a quadrilateral with $0 < l_2 < \pi/4$ determined by

$$\cos^2 2l_2 = \cos^2(\pi/2 - \beta)\sin^2 2r + \cos^2 2r, \tag{14}$$

and $0 < t_2 < \pi/2$ and $s - s_1 < \pi/2 - \beta$ given by (10) and (9). Consequently, the quadrilaterals Γ_2 form a family which is continuous in (l_1, r). By Lemma 12 this gives a truncated rectangular pentagon contour.

We now want to show that all pairs l_1, l_2 with $l_1 + l_2 \leq \pi/4$ are attained, such that there are two different pentagons for $l_1 + l_2 < \pi/4$, and one if equality holds. For this we consider the extremal choices of r. If $r \searrow l_1$ then by (13) $\beta \nearrow \pi/2$, and thus by (14) $l_2 \searrow 0$. On the other hand, for $r = \pi/4$, (13) implies $\beta = 2l_1$, and from (14) we conclude $2l_2 = \pi/2 - 2l_1$.

For given l_1, it follows from continuity that a choice of r in the lower interval $(l_1, \pi/4]$ gives all $l_2 \in (0, \pi/4 - l_1]$. Taking r-derivatives of (13) and (14) it is elementary to see that the function $l_2(r)$ is strictly monotonic. Thus each l_2 in $(0, \pi/4 - l_1]$ is taken exactly once, and in particular $l_1 + l_2 \leq \pi/4$.

The upper r-interval $[\pi/4, \pi/2 - l_1)$ also yields quadrilaterals Γ_2 with $l_2 \in (0, \pi/4 - l_1]$. This follows with the same arguments since the limit $r \nearrow \pi/2 - l_1$ is analogous to $r \searrow l_1$. □

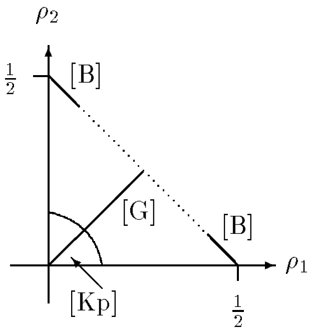

FIGURE 4. The moduli space of rectangular boundary contours can be represented by a two-sheeted covering of the triangle defined by $\rho_1, \rho_2 > 0$ and $\rho_1 + \rho_2 < 1/2$; the two sheets are glued along the dotted line $\rho_1 + \rho_2 = 1/2$.

Fixing the pentagon at p we extend the lengths t_1, t_2 and s to infinity. We denote by $\mathcal{G}$ the family of extended contours which results this way from $\mathcal{G}_{\text{trunc}}$. Although there are many other choices of pentagons for rectangular surfaces besides the family $\mathcal{G}_{\text{trunc}}$, the extended contours are unique. This follows from the decomposition of the pentagon into quadrilaterals (Lemma 12), with the Uniqueness Lemma 10. Furthermore, on the boundary of $\mathcal{G}_{\text{trunc}}$ the lengths l_1 or l_2 vanish. Thus the family $\mathcal{G}$ is maximal:

Theorem 14. *The neckradii $\rho_1, \rho_2 > 0$ of a rectangular 4-unduloid satisfy*

$$\rho_1 + \rho_2 \leq \frac{1}{2}. \tag{15}$$

Furthermore, all rectangular 4-unduloids have a fundamental domain associated to a spherical minimal surface with boundary in the two-dimensional family $\mathcal{G}$ homeomorphic to an open disk; there are two contours which satisfy (15) *with strict inequality, and one for equality.*

The boundary of the moduli space is given by the contours with vanishing ρ_1 or ρ_2; the degenerate limiting contours bound surfaces associated to Delaunay surfaces with an orthogonal string of spheres.

We believe that our two-parameter family $\mathcal{G}$ is in 1-1 correspondence to a continuous family of rectangular CMC surfaces. One sheet of the boundary contours with $r > \pi/4$ corresponds to *spheroidal* surfaces with more spherical centers, while for the *noidal* surfaces on the other sheet with $r < \pi/4$ the centers are smaller. In particular a rescaled sequence of surfaces in the latter sheet with $\rho_1 = \lambda\rho_2 \to 0$ converges to a minimal surface with four catenoid ends of alternating logarithmic growth.

To prove existence, one would have to solve Plateau's problem for the spherical contours in $\mathcal{G}$ with minimal surfaces. We believe these minimal surfaces are unique, at least in the class with almost embedded associate surfaces. So far existence is known for the following cases (see Figure 4):

- On an infinite subset with accumulation point the origin $\rho_1 = \rho_2 = 0$ by Kapouleas [Kp]. It is conceivable that these spheroidal surfaces form in fact an open continuous family (cf. Remark 4.6 of [Kp]).

- On the diagonal of $\mathcal{G}$ where the corresponding dihedrally symmetric 4-unduloids attain the neckradii $0 < \rho_1 = \rho_2 \le 1/4$ [G].
- Existence of the maximal neckradius family with $\rho_1 + \rho_2 = 1/2$ for either ρ_1 or ρ_2 small was shown by Berglund [B]. Asymptotically, these surfaces are almost cylinders in one direction, and almost spherical unduloids in the other.

It is known that there are only finitely many components in the moduli space of rectangular surfaces with neckradius greater than any fixed $\varepsilon > 0$; this follows from the curvature and area bounds of [KK].

Doubly periodic surfaces of rectangular type. Using Kapouleas' method [Kp], doubly periodic surfaces with rectangular lattice can be found. Here we want to let the lattice size vary, and require only that rectangular symmetry is maintained (we still fix $H = 1$). Under this assumption Kapouleas has countably many families $\mathcal{F}_{m,n}$, each accumulating at the following degenerate surfaces: on one set of parallel axes there are $m \ge 0$ spheres in between the junction spheres and likewise $n \ge 0$ spheres in a perpendicular direction. The boundary of the associated minimal fundamental domains form a family of contours $\mathcal{G}_{m,n}$. This family is obtained from $\mathcal{G}_{\text{trunc}}$ as follows: for a contour in $\mathcal{G}_{\text{trunc}}$ the arc t_1 is extended by $n\pi/2$, t_2 by $m\pi/2$, and s by $(m+n)\pi/2$.

Since a continuous family of CMC surfaces gives rise to a continuous family of associated spherical boundary polygons (Lemma 4) the maximality of $\mathcal{G}_{\text{trunc}}$ gives the maximality of $\mathcal{G}_{m,n}$:

Theorem 15. *For each $m, n \ge 0$, Kapouleas' doubly periodic rectangular surfaces $\mathcal{F}_{m,n}$ are contained in a different connected component of the moduli space of doubly periodic surfaces with rectangular symmetry.*

We believe that the Plateau problem for the contours $\mathcal{G}_{m,n}$ can be solved with a continuous family of surfaces extending those of Kapouleas, so that $\mathcal{G}_{m,n}$ would be homeomorphic to the CMC moduli space.

The numerical results of [GP] make us doubt that the theorem continues to hold in the class of all (not necessarily rectangular) doubly periodic surfaces. Rather, it seems that only the imposition of a sufficiently strong symmetry group separates the moduli space into different connected components.

5. Isosceles triunduloids

The class $\mathcal{M}_{g,3}$ of triunduloids of any genus is special in that a (horizontal) symmetry plane is present [KKS]. Indeed by balancing (4) the three force vectors of the ends must be contained in a plane, which is a symmetry plane by Corollary 6(i). We assume an additional orthogonal (vertical) symmetry plane and call the triunduloids of this type *isosceles*. The intersection of the two symmetry planes contains the axis of one end, which we call the *stem*. The other two ends are congruent, and their axes, the *arms*, enclose a well-defined angle

$$\alpha \in (0, \pi/2)$$

with the intersection of the symmetry planes (see Figure 1(b)). The case $\alpha = 0$ is impossible by Corollary 6(ii). Angles $\pi/2 \le \alpha \le \pi$ are excluded by the balancing formula (4); we remark that isosceles triunduloids with $\pi/2 < \alpha < \pi$ exist outside the almost embedded class, for instance with nodoid ends on either stem or arms [Kp].

As with the symmetric 4-unduloids in the previous section, we can characterize a fundamental domain for any isosceles triunduloid of genus 0. The conformal model in Subsection 2.2 lets us represent either half of a triunduloid as a closed disk with three boundary punctures, and the vertical reflection must fix one of the punctures and interchange the other two. It follows from Lemma 7 that the fixed point set of the vertical reflection consists of a geodesic curvature line symmetric about the horizontal mirror plane and meeting it only at some point $\tilde{p}$. Each symmetric half of this line is a ray from $\tilde{p}$ running out the stem. Besides one such ray in the vertical plane, a fundamental domain for any isosceles triunduloid is bounded by a geodesic curvature ray and line in the horizontal plane (see Figure 5(a)).

Again the known asymptotics of the ends allows us to truncate the associated infinite contour with its asymptotic perpendiculars. Starting with the point p associated to $\tilde{p}$ (Figure 5) the Hopf fields of the truncated contour can be seen to be $-B$ (ray of half end), $\cos\alpha\, A - \sin\alpha\, C$ (asymptotic perpendicular for half end), $-B$ (line), $-A$ (asymptotic perpendicular of quarter end), C (ray). We can require

$$0 < l \leq \frac{\pi}{4} \qquad \text{and} \qquad 0 < r \leq \frac{\pi}{2}, \tag{16}$$

if we truncate the contour with the shorter geodesics, i.e. we cap the ends at the necks not at the bubbles. We call a pentagon with the above Hopf fields which satisfies (16) a *truncated isosceles contour* and denote it with its five lengths $\Gamma(b, r, s-b, l, t)$.

5.1. **Trigonometry.** Like the rectangular case, the main idea is to reduce the trigonometry of the pentagons to quadrilaterals. In this case one of the two quadrilaterals in the decomposition is what we call a *Clifford rectangle* $\Gamma_C(b, r)$. This is a right-angled quadrilateral of edgelength b and r which is subset of a Clifford torus. Opposite arcs are Clifford parallel, and the Hopf fields can be taken as A, $-B$, $-A$, $\cos(2b)B - \sin(2b)C$. Thus in the special case $b = \pi/4$ a Clifford rectangle is also a rectangular Lawson quadrilateral of the type in Lemma 9(*iii*). In the general case the Hopf fields are easily derived from those of a Clifford torus (see [G]).

Lemma 16. (*i*) *A Lawson quadrilateral* $\Gamma_L(l, t, r, s; \pi/2 - \alpha + 2b)$ *and a Clifford rectangle* $\Gamma_C(b, r)$ *can be combined to form a truncated isosceles contour* $\Gamma(b, r, s-b, l, t)$ *if condition* (16) *and the following hold:* $s > b$, *and* $0 < \pi/2 - \alpha + 2b < \pi$.
(*ii*) *Conversely, a pentagon satisfying* (16) *and* $k\pi < s - b, t < (k+1)\pi$ *for sufficiently large* $k \in \mathbb{Z}$ *can be decomposed into a Lawson quadrilateral and a Clifford rectangle as in* (*i*).

Proof. (*i*) If the Clifford rectangle is glued to the Lawson quadrilateral such that the b-arc of the rectangle is subset of the s-arc of the quadrilateral, and the r-arcs agree (as indicated in Figure 5), then a pentagon for isosceles surfaces results.

(*ii*) We construct a great circle arc through the point p which meets the opposite $-B$ geodesic line orthogonally. Since both rays of the half end have the same $-B$ Hopf field, they have a continuous set of perpendiculars which are all Clifford parallel to the r-arc. Thus a Clifford parallel to the r-arc (in the orientation indicated in Figure 5) at distance b gives a diagonal with Hopf field $\cos(\alpha - 2b)\, A - \sin(\alpha - 2b)\, C$. We have to go the same distance b on both $-B$ arcs to obtain

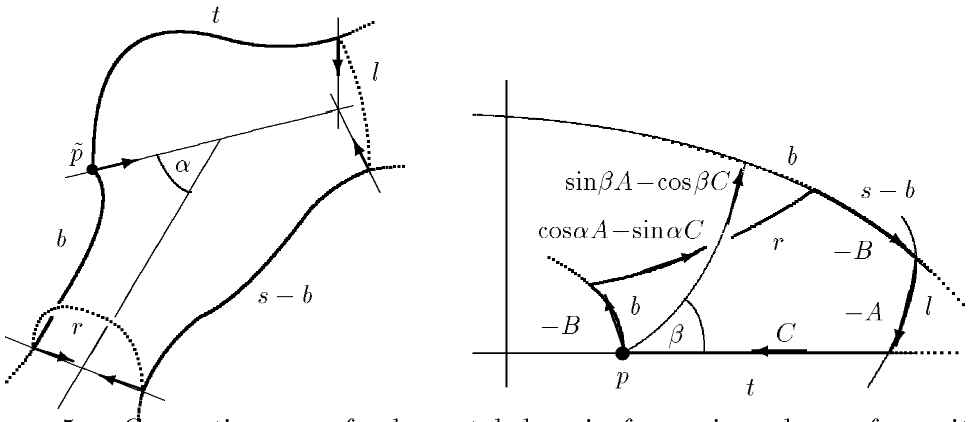

FIGURE 5. Generating CMC fundamental domain for an isosceles surface with dotted asymptotic curvature lines, and spherical boundary polygon of associated spherical minimal surface truncated with the asymptotic perpendiculars.

the Clifford rectangle of the r-arc and the diagonal; this means that the diagonal only meets an extension of the opposite $-B$ arc.

Writing the Hopf field of the diagonal in the form $\sin(\pi/2-\alpha+2b)\,A-\cos(\pi/2-\alpha+2b)\,C$ we see that the other quadrilateral formed has only one non-right angle

$$\beta := \frac{\pi}{2} - \alpha + 2b$$

at p and hence is a Lawson quadrilateral. □

The problem to determine the possible neckradii amounts to investigating how the length l of the asymptotic perpendicular truncating the quarter end (stem) relates to the length r of the perpendicular truncating the half end (arms). For the Lawson quadrilateral $\Gamma_L(l,t,r,s;\pi/2-\alpha+2b)$ we obtain from (11) an expression involving the length b,

$$\cos^2 2l = \sin^2(\alpha-2b)\sin^2 2r + \cos^2 2r. \tag{17}$$

5.2. **Balancing and the period problem.** There is a period problem for isosceles surfaces: the associated CMC domain must have the two rays bounding the half end in the *same* plane, not just in parallel planes. Boundary contours which can bound surfaces with vanishing periods form a codimension one family within all truncated isosceles contours. Although we do not give an existence proof, we can select such a family using two facts: the balancing formula, and the asymptotics of the ends. Technically the condition we obtain is a further necessary condition on the boundary contours.

The balancing formula (4) relates the forces f^A of the arms to the force f^S of the stem

$$|f^S| = 2\cos\alpha\,|f^A|.$$

Thus (3) yields for the asymptotic neckradii ρ^S and ρ^A

$$2\pi\rho^S(1-\rho^S) = 2\cos\alpha\,2\pi\rho^A(1-\rho^A).$$

The arc lengths of the perpendiculars in the truncated contour are related to the neckradii,

$$2\pi\rho^S = 4l \qquad \text{and} \qquad 2\pi\rho^A = 2r, \tag{18}$$

and we obtain

$$l(\pi - 2l) = \cos\alpha\, r(\pi - r).$$

Solving this quadratic equation for those l admissible by (16) we arrive at the following statement on the pentagon lengths, which, by (18) is in fact a result on the neckradii.

Lemma 17. *Let Γ be the contour bounding a minimal surface in $\mathbb{S}^3$ associated to the fundamental domain of a (balanced) isosceles surface. If the great circle rays of the half end in Γ have a shortest perpendicular with length r, then the great circle rays of the quarter end have shortest perpendiculars of length*

$$0 < l = \frac{\pi}{4} - \sqrt{\frac{\pi^2}{16} - \cos\alpha\,\frac{r(\pi - r)}{2}} \le \frac{\pi}{4}. \tag{19}$$

In particular, (19) has only a solution for those $0 \le r \le \pi/2$ which are not greater than

$$r_{\max}(\alpha) := \begin{cases} \frac{\pi}{2}\left(1 - \sqrt{1 - \frac{1}{2\cos\alpha}}\right) & \text{for} \quad 0 < \alpha \le \frac{\pi}{3} \\ \frac{\pi}{2} & \text{for} \quad \frac{\pi}{3} \le \alpha < \frac{\pi}{2}. \end{cases}$$

5.3. **Truncated associated boundary contours.** We now study the truncated isosceles contours via the Decomposition Lemma 16. The first step is to describe a family of quadrilaterals satisfying (17) and (19). Eliminating l from these equations means that (α, r, b) is a zero of the function

$$f(\alpha, r, b) := \sin^2(\alpha - 2b)\sin^2 2r + \cos^2 2r - \sin^2\sqrt{\frac{\pi^2}{4} - 2\cos\alpha\, r(\pi - r)}.$$

Conversely, a zero (α, r, b) of f and the length l defined by (19) solve (17). We now want to determine all zeros of f. By the periodicity of f in b it will be sufficient to confine b to some interval of length π. Specifically, we set

$$\Omega := \left\{(\alpha, r, b) \mid 0 < \alpha < \pi/2,\ 0 < r \le r_{\max}(\alpha),\ \frac{\alpha}{2} - \frac{\pi}{4} \le b \le \frac{\alpha}{2} + \frac{\pi}{4}\right\}.$$

Lemma 18. *On the set Ω, all zeros of f form a continuous two-parameter family homeomorphic to an open disk*

$$\mathcal{D} := \{(\alpha, r, b) \in \Omega \mid 0 < r \le R(\alpha), b = b_i(\alpha, r) \ \text{for} \ \ i = 1, 2\},$$

where

$$R(\alpha) := \pi\frac{1 - \cos\alpha}{2 - \cos\alpha}.$$

Here $b_1(\alpha, r) \in (\alpha/2 - \pi/4, \alpha/2]$ and $b_2(\alpha, r) \in [\alpha/2, \alpha/2 + \pi/4)$ are two continuous functions with $b_1(\alpha, R(\alpha)) = b_2(\alpha, R(\alpha)) = \alpha/2$.

Proof. It is straightforward to show that $f(\alpha, r, b)$ is defined on Ω, i.e. $R(\alpha) \le r_{\max}(\alpha)$. We want to find zeros of f on Ω. We establish $b_1(\alpha, r)$ first for r in the open interval $0 < r < R(\alpha)$. An explicit formula for $b_1(\alpha, r)$ involves many square roots, so it is more straightforward to apply the implicit function theorem. To do so we claim:

(i) $\frac{\partial f}{\partial b} < 0$ on Ω,

(ii) $f(\alpha, r, \alpha/2 - \pi/4) > 0$ for $0 < \alpha < \pi/2$ and $0 < r \le R(\alpha)$, and

(iii) $f(\alpha, r, \alpha/2) < 0$ for $0 < \alpha < \pi/2$ and $0 < r < R(\alpha)$.

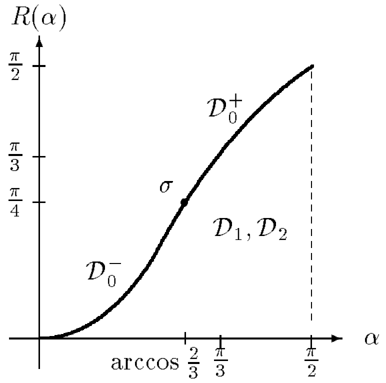

FIGURE 6. The function $R(\alpha)$ and the projection of $\mathcal{D}$.

The derivative

$$\frac{\partial f}{\partial b} = -2\sin(2\alpha - 4b)\sin^2 2r \tag{20}$$

is clearly negative on Ω which gives claim (i). To prove (ii) observe $\sin^2(\alpha - 2(\alpha/2 - \pi/4)) = 1$, so we have $f(\alpha, r, \alpha/2 - \pi/4) = \sin^2 r + \cos^2 r - \sin^2\left(2\sqrt{\frac{\pi^2}{16} - \cos\alpha\frac{r(\pi - r)}{2}}\right) = \cos^2(2\sqrt{\ldots})$. This is non-negative and vanishes exactly at $r = 0$.

Proving (iii) amounts to a further elementary calculation: $f(\alpha, r, \alpha/2) < 0$ is equivalent to

$$\sin^2\left(\frac{\pi}{2} - 2r\right) < \sin^2\sqrt{\frac{\pi^2}{4} - 2\cos\alpha r(\pi - r)}.$$

Since $0 < \sqrt{\ldots} < \pi/2$ and $-\pi/2 < \pi/2 - 2r < \pi/2$ this is equivalent to

$$\left|\frac{\pi}{2} - 2r\right| < \sqrt{\frac{\pi^2}{4} - 2\cos\alpha r(\pi - r)}.$$

Squaring yields

$$\frac{\pi^2}{4} - 2r(\pi - 2r) < \frac{\pi^2}{4} - 2\cos\alpha r(\pi - r),$$

which is equivalent to $\pi - 2r > \cos\alpha(\pi - r)$, $\pi(1 - \cos\alpha) > (2 - \cos\alpha)r$ or, finally, $0 < r < R(\alpha)$.

For each α the implicit function theorem gives a differentiable function $b_1(\alpha, r)$ where $0 < r < R(\alpha)$. The function b_1 is unique in the subset of Ω with $\pi/4 - \alpha/2 < b < \alpha/2$ by (i).

It is a direct consequence of the previous calculation that $(\alpha, R(\alpha), \alpha/2)$ is also a zero of f. Moreover from (20) it follows that this is the only zero in Ω with $r = R(\alpha)$ and $b \le \alpha/2$. Thus we can continuously extend b_1 by setting $b_1(\alpha, R(\alpha)) = \alpha/2$. Furthermore, if $r > R(\alpha)$ it follows from the calculation that $2\sqrt{\pi^2/4 - 2\cos\alpha r(\pi - r)} < |\pi/2 - 2r|$; thus $f(\alpha, r, b) > \sin^2(\alpha - 2b)\sin^2 2r > 0$, and there are no zeros of f for $r > R(\alpha)$.

To obtain $b_2 \in [\alpha/2, \pi/4)$ we set $b_2(\alpha, r) := \alpha - b_1(\alpha, r)$. Then $\alpha - 2b_1 = 2b_2 - \alpha$ and this leaves f is invariant. All properties claimed for b_2 follow from b_1. $\square$

To determine the Lawson quadrilaterals in the form for Lemma 16, we have to select values of l, t, and s satisfying (5) – (8). Whereas there is a continuous way to choose l, the two lengths t and s which reflect the position of the truncation by the asymptotic perpendiculars must have a discontinuity on $\mathcal{D}$. In the following lemma we first establish the quadrilaterals on $\mathcal{D}_i = \{(\alpha, b, r) \in \mathcal{D} \mid b = b_i(\alpha, r), r \neq R(\alpha)\}$ for $i = 1, 2$, and $\mathcal{D}_0 := \{(\alpha, \alpha/2, R(\alpha))\}$. Then we discuss the continuity problem. It will be useful to decompose $\mathcal{D}_0$ further, namely into the two sets $\mathcal{D}_0^- := \{(\alpha, b, r) \in \mathcal{D}_0 \mid \alpha < \arccos(2/3)\}$ and $\mathcal{D}_0^+ := \{(\alpha, b, r) \in \mathcal{D}_0 \mid \alpha > \arccos(2/3)\}$, as well as the point $\sigma := (\arccos(2/3), \arccos(2/3)/2, \pi/4)$. We can now state the main technical lemma for the isosceles case.

Lemma 19. *For each point $(\alpha, b, r) \in \mathcal{D} - \{\sigma\}$ there is a Lawson quadrilateral $\Gamma_L(l, t, r, s; \pi/2 - \alpha + 2b)$ satisfying* (17), (19), *and* (16). *According to the decomposition of $\mathcal{D} - \{\sigma\}$ into $\mathcal{D}_1 \cup \mathcal{D}_2 \cup \mathcal{D}_0^\pm$ we write the families of these quadrilaterals as $\mathcal{G}_1 \cup \mathcal{G}_2 \cup \mathcal{G}_0^\pm$. Moreover, these quadrilaterals are unique with $0 < s, t \leq \pi$. For the point σ there is a one parameter family of distinct quadrilaterals $\mathcal{G}_0^\sigma$ with $0 < s, t \leq \pi$. The length l of all these quadrilaterals induces a continuous function on $\mathcal{D}$, which vanishes on $\partial\mathcal{D}$. The lengths t, s are continuous on $\mathcal{D}_1 \cup \mathcal{D}_0^+ \cup \mathcal{D}_2$. When $(\alpha, r, b) \in \mathcal{D}_2$ approaches a point in $\mathcal{D}_0^-$, we have* $\lim s = \lim t = \pi$*; whereas for $(\alpha, r, b) \in \mathcal{D}_1$ approaching such a point,* $\lim s = \lim t = 0$.

Proof. A unique value $0 < l \leq \pi/4$ on $\mathcal{D}$ is determined by (19). Since r and α are continuous on $\mathcal{D}$ so is l. On the portion of $\partial\mathcal{D}$ with $r = 0$ it follows that $l \equiv 0$. The remaining boundary of $\mathcal{D}$ satisfies $\alpha = \pi/2$. Again, it follows directly from (19) that $l \searrow 0$ when this boundary arc is approached.

(i) We now want to define s, t on $\mathcal{D}_1 \cup \mathcal{D}_2$. For the points in $\mathcal{D}_1$ with $b_1 < \alpha/2$ we have $0 < \beta < \pi/2$. In this case (10) and (9) define $0 < s, t < \pi/2$ continuously, and uniquely within $(0, \pi]$. This gives $\mathcal{G}_1$.

In the proof of Lemma 8 we pointed out that the following substitution is a bijection of Lawson quadrilaterals:

$$(l, r, s, t; \beta) \mapsto (l, r, \pi - s, \pi - t; \pi - \beta). \tag{21}$$

When we take the quadrilaterals $\mathcal{G}_1$, this substitution gives quadrilaterals $\mathcal{G}_2$ parameterized by $\mathcal{D}_2$ with $\pi/2 < \beta < \pi$ and unique lengths $\pi/2 < s, t < \pi$.

(ii) We now discuss the case $b = \alpha/2$ or $\beta = \pi/2$. On $\mathcal{D}_0^-$ we have $R(\alpha) < \pi/4$. From (17) follows $\cos^2 2l = \cos^2 2R(\alpha)$, so that $l = R(\alpha)$ by (16). This satisfies (19) too, thus the Lawson quadrilaterals are of the form $\Gamma(R(\alpha), t, R(\alpha), s; \pi/2)$. Lemma 9($ii$) gives the one-parameter family $\Gamma(R(\alpha), \pi, R(\alpha), \pi; \pi/2)$ defining $\mathcal{G}_0^-$. By Lemma 10 these are all such Lawson quadrilaterals with $0 < s, t \leq \pi$.

On $\mathcal{D}_0^+$ we have $R(\alpha) > \pi/4$ and $l = \pi/2 - R(\alpha)$ satisfies (19). Now Lemma 9(i) gives the quadrilaterals $\Gamma(\pi/2 - R(\alpha), \pi/2, R(\alpha), \pi/2; \pi/2)$ which are again unique. These give the family $\mathcal{G}_0^+$.

Finally, at the point σ with $R(\alpha) = l = \pi/4$ there is an entire one-parameter family $\mathcal{G}_0^\sigma$ of unique quadrilaterals $\Gamma(\pi/4, s, \pi/4, s; \pi/2)$ with $0 < s < \pi$ given by Lemma 9(iii). This proves (ii).

We have to compare the quadrilaterals of (ii) with the one-sided limits taken in $\mathcal{D}_1$ and $\mathcal{D}_2$. The points of $\mathcal{D}_1$ converging to $\mathcal{D}_0^-$ are of the form $(\alpha, r, b_1(\alpha, r))$ with $\alpha < \arccos(2/3)$. Thus for

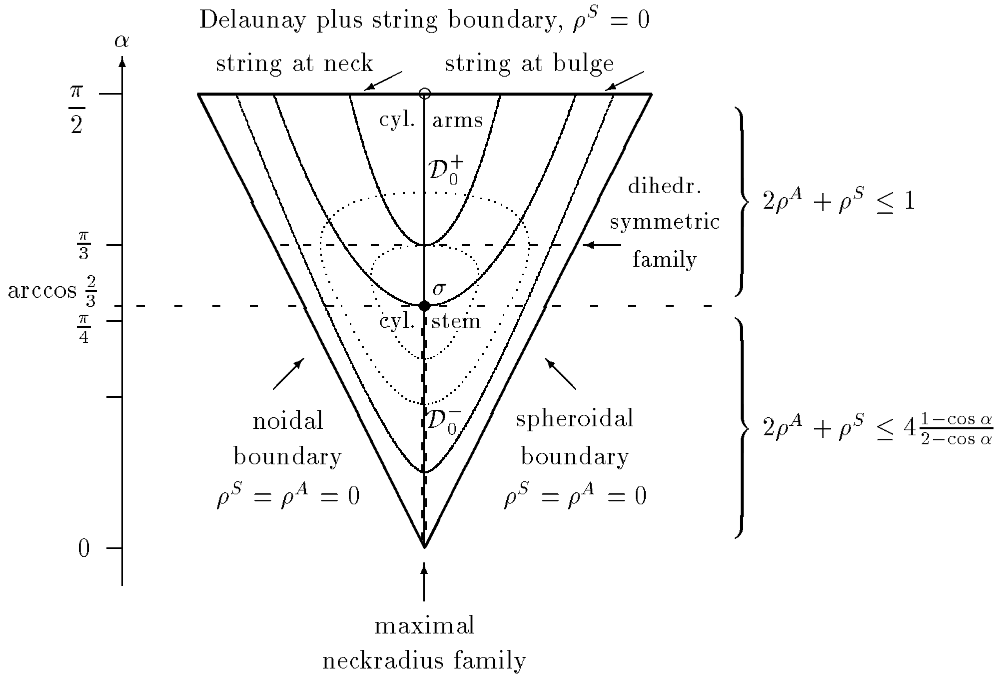

FIGURE 7. The moduli space of the isosceles boundary contours represented schematically as the interior of a triangle. We indicate some curves of constant neckradius with solid lines for the arms, and dotted lines for the stem. Existence is only proved for the dihedrally symmetric family [G] and in an infinite set in a neighborhood of the spheroidal boundary [Kp].

$r \nearrow R(\alpha)$ we find $t \searrow 0$ by (10) and $s \searrow 0$ by (9). On the other hand the limits from $\mathcal{D}_2$ (given by the b_2 branch through the substitution (21) from the b_1 values) have $s, t \nearrow \pi$.

However, for the limits converging to $\mathcal{D}_0^+$ we obtain continuity: the limiting quadrilaterals with (α, r, b_1) for $r \nearrow R(\alpha) > \pi/4$ have $t \nearrow \pi/2$ by (10), and $s \nearrow \pi/2$ by (9). The same lengths are obtained for the similar limit with (α, r, b_2) via (21). □

5.4. **All isosceles boundary contours.** The truncated pentagons one obtains by applying Lemma 16 to the family of quadrilaterals constructed in Lemma 19 have an arc with (formal) length $s - b$, which may be negative. This could be avoided by taking s sufficiently large. Instead, we extend the arcs with lengths b, t, $s-b$ to infinity, and obtain the boundary contours for isosceles surfaces directly from the quadrilaterals. The infinite contours no longer have a discontinuity along $\mathcal{D}_0^-$.

Theorem 20. *An isosceles surface of angle $0 < \alpha < \pi/2$ and with neckradii (ρ^S, ρ^A) satisfies*

$$\rho^A \leq \rho^A_{\max}(\alpha) := \tfrac{1-\cos\alpha}{2-\cos\alpha}, \tag{22}$$

$$\rho^S \leq \rho^S_{\max}(\alpha) := \min\left\{\tfrac{\cos\alpha}{2-\cos\alpha}, 1 - \tfrac{\cos\alpha}{2-\cos\alpha}\right\} \quad . \tag{23}$$

Furthermore, each fundamental domain of an isosceles surface is associated to a minimal domain in $\mathbb{S}^3$ with boundary contained in a family $\mathcal{G}$, which is homeomorphic to a two-dimensional open *disk. Each pair of neckradii satisfying the strict inequalities in* (22) *and* (23) *arises for two different boundary contours in* $\mathcal{G}$, *and equality is satisfied with one contour. On* $\partial\mathcal{G}$ *the contours degenerate with* $\rho^S = 0$.

In particular the neckradius sum over all three ends satisfies

$$2\rho^A + \rho^S \le \min\left(1, 4\,\frac{1-\cos\alpha}{2-\cos\alpha}\right). \tag{24}$$

Proof. If we extend s and t of the quadrilaterals $\mathcal{G}_1 \cup \mathcal{G}_2 \cup \mathcal{G}_0^{\pm} \cup \mathcal{G}_0^{\sigma}$ (from Lemma 19) by π then Lemma 16 gives non-degenerate pentagons. The family $\mathcal{G}$ is now obtained by extending the arcs of the pentagon with length t, b, and $s-b$ to infinity. This extension leads to the same boundary contour for all contours in $\mathcal{G}_0^{\sigma}$, and thus $\mathcal{G}$ is parameterized by the disk $\mathcal{D}$. Furthermore, this parameterization is continuous since l, r are continuous by Lemma 19.

The family $\mathcal{G}$ contains all isosceles boundary contours, since truncation of a such a contour leads to a pentagon for isosceles surfaces. For these we can assume $0 < s, t \le \pi$ if we move the perpendiculars and then but uniqueness follows from the uniqueness of quadrilaterals stated in Lemma 19. □

Again we expect a continuous family of isosceles CMC surfaces to be in a 1-1 relation to our boundary contours. Existence is known in two cases:

- For an infinite set accumulating in the spheroidal boundary arc with $\rho^S = \rho^A = 0$ (see 5.5.1 below) [Kp], and
- for the one-parameter subfamily of dihedrally symmetric triunduloids with $\alpha = \pi/3$ by [G].

5.5. **The geometry of the isosceles family.** On the assumption that our family of contours is bijective to a family of CMC surfaces, we discuss the geometrical properties of this family. Using a numerical existence scheme, we found such a two parameter family of isosceles surfaces, and give images in the paper [GP].

5.5.1. *The moduli space boundary.* There are three geometrically distinguished arcs on the boundary of isosceles contours, i.e. the contours parameterized with $\partial\mathcal{D}$. All contours on the boundary have vanishing neckradius of the stem end.

On the *spheroidal boundary*, parameterized with $(\alpha, 0, \alpha) \in \partial\mathcal{D}$ we have $\rho^S = \rho^A = 0$, so that the limiting configuration consists of strings of spheres with isosceles symmetry. The limiting lengths (mod π) of the curvature arcs are $t = \pi$, $b = \alpha$, and $s - b = \pi - \alpha$; considered as real numbers they describe the lengths on the central junction sphere with punctures at the limit points of the necks. Kapouleas' method [Kp] gives isosceles surfaces, which accumulate at the spheroidal boundary arc.

On the *noidal boundary*, parameterized with $(\alpha, 0, 0)$, the ends are also spherical ($\rho^S = \rho^A = 0$) but the contours have $b = t = 0$. This is the expected value for noidal junctions, i.e. the three strings of spheres are attached to a point. A blow-up in the center of the CMC surfaces such that the necks are scaled to constant radius gives in the limit a minimal trinoid with isosceles symmetry. The existence of k-unduloids close to this noidal boundary component might follow from analogous work in the constant scalar curvature setting [MP].

The noidal and spheroidal boundary agree in a limiting contour with $\alpha = 0$. In this degenerate case the two arms coincide and form a double string of spheres.

Finally there is an arc on $\partial\mathcal{D}$ with $\alpha = \pi/2$ which we call *Delaunay plus string.* Here only $\rho^S = 0$, but $\rho^A \in (0, \pi/2]$. For the half with $b < \alpha/2$, there is a string of spheres attached to a Delaunay neck. When $\rho^A \to 0$ the Delaunay surface itself tends to a string of spheres, and the limit agrees with the noidal boundary case for $\alpha = \pi/2$. At the other endpoint, $\rho^A \to \pi/2$ the Delaunay surface is a cylinder. This leads over to the other half of the family with $b > \alpha/2$ which is a similar family with the string of spheres attached at a Delaunay bubble. Its limiting case is spheroidal.

5.5.2. *A triunduloid with one cylindrical end.* The contour at $\sigma \in \mathcal{D}$ has arm neckradius $\rho^A = 1/4$ and the stem has the cylindrical neckradius $\rho^S = 1/2$. The arms enclose an angle of $2\arccos(2/3) \approx 96.4°$. This is the only contour in the family with a cylindrical neckradius. The arms can attain the cylindrical neckradius only on the moduli space boundary.

5.5.3. *The maximal neckradius family.* This one-parameter subfamily of contours in $\mathcal{G}$ is parameterized by $\mathcal{D}_0$ and realizes the maximal neckradii for a given α. It includes the contour with cylindrical stem. The right hand side of (23) gives the minimal and maximal asymptotic radius of the stem; on $\mathcal{D}_0^-$ the first radius is minimal, while on $\mathcal{D}_0^+$ the second one is. At the cylindrical contour the minimum flips and the consequence is the non-differentiability of the maximal neckradius sum (24) at σ: the neckradius sum is 1 for $\arccos(2/3) \leq \alpha < \pi/2$, but smaller than 1 for $0 < \alpha < \arccos(2/3)$. If we replace the neckradius ρ^S by the asymptotic bulgeradius $\rho_0^S = \cos\alpha/(2 - \cos\alpha)$ then $2\rho^A + \rho_0^S = 1$ on the maximal family.

It is interesting to observe that the asymptotic position of the minimum neckradius shifts by $\pi/2$ at σ, so that the selection of an asymptotic planar curvature circle of radius ρ^S can not be analytic. Indeed, our values $s \bmod \pi$, $t \bmod \pi$ given by Lemma 19 are discontinuous on the maximal neckradius family at σ, when they jump by $\pi/2$, half a translational period of the end.

5.5.4. *Marked bubbles.* It may appear that selecting a family without requiring (16) would avoid the discontinuity of t and s in our description, so that a perpendicular of the boundary rays could be marked in a continuous way over the family. However, we want to show that a discontinuity must be present around σ.

Let $\gamma \subset \mathcal{D} - \{\sigma\}$ be a loop winding once about the point σ. The isosceles boundary contours are continuous on γ. Nevertheless, according to Lemma 19, the corresponding path of quadrilaterals $\Gamma_L(\gamma)$ has a discontinuity in s, t of $\pm\pi$, when $\mathcal{D}_0^-$ is crossed. Thus the asymptotic perpendicular moves by one full period along the stem. This means that on the closed loop γ a bubble is created or deleted on the stem end. Note also that the discontinuity of t, s can be located on a curve joining any point of $\partial\mathcal{D}$ to σ.

As a consequence, a closed curve winding n times about σ generates or deletes $|n|$ bubbles on the stem. For all isosceles surfaces, except for the one with cylindrical stem, we can mark a bubble on the stem. The corresponding "marked" moduli space is then the universal covering of the annulus $\mathcal{D} - \{\sigma\}$.

References

[A] A.D. Alexandrov: Uniqueness theorems for surfaces in the large. V, Vestnik Leningrad University, **19(13)** (1958), 5–8, English translation in Amer. Math. Soc. Transl. (Series 2) **21**, 412–416 (1962)

[B] J. Berglund: Dissertation, University of Massachusetts, Amherst, 1996

[G] K. Große-Brauckmann: New surfaces of constant mean curvature, Math. Zeit. **214**, 527–565 (1993)

[GP] K. Große-Brauckmann, K. Polthier: Constant mean curvature surfaces derived from Delaunay's and Wente's surfaces, in: Visualization and Mathematics (H.-C. Hege and K. Polthier, eds.), Springer Berlin (1997)

[GKS] K. Große-Brauckmann, R.B. Kusner, J.M. Sullivan: Embedded CMC surfaces with three ends. Preprint 1997

[Ka] H. Karcher: The triply periodic minimal surfaces of A. Schoen and their constant mean curvature companions, Man. math. **64**, 291–357 (1989)

[Kp] N. Kapouleas: Complete constant mean curvature surfaces in Euclidean three-space, Ann. of Math. **131**, 239–330 (1990)

[KKn] N. Korevaar, R. Kusner: Asymptotic necksize bounds for CMC surfaces. Notes 1990

[KK] N. Korevaar, R. Kusner: The global structure of constant mean curvature surfaces, Invent. Math. **114**, 311–332 (1993)

[KKS] N. Korevaar, R. Kusner, B. Solomon: The structure of complete embedded surfaces with constant mean curvature, J. Diff. Geom. **30**, 465–503 (1989)

[K1] R. Kusner: Bubbles, conservation laws, and balanced diagrams. In: Geometric analysis and computer graphics (P. Concus, R. Finn, D. Hoffman, eds.), 103–108, Springer New York 1990

[K2] R. Kusner: Natural Lagrangian and symplectic structures for moduli spaces of CMC surfaces and CSC metrics. Preprint 1997

[KMP] R. Kusner, R. Mazzeo, D. Pollack: The moduli space of complete embedded constant mean curvature surfaces, Geom. Funct. Anal. **6**, 120–137 (1996)

[L] H.B. Lawson: Complete minimal surfaces in $\mathbb{S}^3$. Ann. of Math. **92**, 335–374 (1970)

[MP] R. Mazzeo, F. Pacard: Constant scalar curvature metrics with isolated singularities. Preprint 1996

[M] W.H. Meeks: The topology and geometry of embedded surfaces of constant mean curvature, J. Diff. Geom. **27**, 539–552 (1988)

Universität Bonn, Mathematisches Institut, Beringstr. 1, 53115 Bonn, Germany

E-mail address: kgb@math.uni-bonn.de

Mathematics Department, University of Massachusetts, Amherst MA 01003, USA

School of Mathematics, Institute for Advanced Study, Princeton NJ 08540, USA

E-mail address: kusner@math.umass.edu